Sakarya Üniversitesi Fen Bilimleri Dergisi
Sakarya University Journal of Science

e-ISSN : 2147-835X
Publisher : Sakarya University

Vol. 29, No. 2, 218-225, 2025
DOI: https://doi.org/10.16984/saufenbilder.1414507

Research Article

Densification of CuO-ZrO_2 Nanocomposites by Flash Sintering

Zeynep Çetinkaya[1-2]

[1] Konya Technical University, Department of Metallurgical and Materials Engineering, Konya, Türkiye, zcetinkaya@ktun.edu.tr, ror.org/02s82rs08
[2] University of Colorado Boulder, Department of Mechanical Engineering, Materials Science and Engineering, Boulder, CO, USA, zeynep.cetinkaya@colorado.edu, ror.org/02ttsq026

ARTICLE INFO

Keywords:
CuO/ZrO_2
Conventional sintering
Flash sintering
Hydrothermal synthesis
Nanocomposites

Article History:
Received: 04.01.2024
Revised: 18.02.2025
Accepted: 27.03.2025
Online Available: 15.04.2025

ABSTRACT

This study is a comprehensive investigation into CuO-doped ZrO_2 nanoparticles (NPs) produced by the hydrothermal method and its conventional (CS) and flash-sintering (FS) processes. Besides this production, the effect of the differences in sintering techniques and density was investigated to prove the results. However, to the authors' knowledge, the FS of CuO/ZrO_2 nanocomposite (NC) material has yet to be studied, which is *the first report* on this material. The CuO/ZrO_2 nanocomposite particle (NCP) pellet was sintered at 1250 °C for 1 hour using CS. The other sintering method is FS, which obtains highly dense NCs. The CuO/ZrO_2 NCPs pellet was successfully produced with the lower sintering temperature (673 °C) and duration (60 seconds) by FS under a current density of 50 mA/mm^2, and electric field (100 V/cm). The microstructure and density of the pellets produced from CS and FS experiments were evaluated. The SEM results showed that the CuO/ZrO_2 NCPs with the FS experiment were successfully performed, and density results with 4.38 g/cm^3 proved this success compared to CS pellet density (3.72 g/cm^3). The FS process for CuO/ZrO_2 NCPs consumes ~ 2.2 kJ (0.227 kJ/cm^3), whereas CS samples require ~ 13 kJ (54 kJ/cm^3), making FS approximately six times more energy-efficient. This significant reduction in energy consumption highlights FS as a promising method for future applications focused on carbon emission reduction and energy efficiency.

1. Introduction

Copper and its alloys are ideal candidates due to their excellent thermal and electrical conductivity. Despite these properties, copper exhibits low wear resistance and limited strength. To improve such properties, ceramics are added to the metal composition to produce materials with a new composition and properties. In the literature, these materials with metal-ceramic combinations are called metal-doped composites. Metal-doped materials are widely used in high-performing aerospace, defense, and automotive applications. Since these materials can be found in many variations due to their structure, they can be combined with excellent thermal stability and mechanical properties. Additionally, materials with high electrical and thermal conductivity can be produced for use in various applications [1, 2].

Recently, scientists have investigated various material compositions by enhancing their properties using CuO-doped ceramics with materials such as ZrO_2, Al_2O_3, TiB_2, SiO_2, and graphene [3-5]. This approach has led to extensive research on CuO-doped ZrO_2 ceramics, demonstrating excellent mechanical and physical properties [2, 6-8].

Zirconium dioxide (ZrO_2) is well-known for its high thermal stability, mechanical strength, and excellent ionic conductivity in terms of hardness, photocatalytic degradation, and wear resistance. When doped with materials such as copper, cerium, or yttrium, the properties of zirconia can be further enhanced, resulting in improved structural characteristics and thermal properties.

Cite as: Z. Çetinkaya (2025). Densification of CuO-ZrO2 Nanocomposites by Flash Sintering, *Sakarya University Journal of Science*, 29(2), 218-225. https://doi.org/10.16984/saufenbilder.1414507

This doping process increases the material's resistance to deformation and enhances its overall stability under extreme conditions. These combined properties make ZrO_2 a critical component in various industrial applications, including fuel cell technology and advanced ceramics [9].

CuO/ZrO_2 NCPs have drawn significant attention due to their enhanced functional properties and the broad range of applications [10]. These NCs combine the catalytic efficiency of CuO with the robust structural and thermal properties of ZrO_2. The CuO/ZrO_2 NCPs are notably used in catalysis for reactions such as the benzylation of benzene, where they demonstrate higher catalytic efficiency than individual CuO or ZrO_2 catalysts. This increased efficiency is attributed to the synergistic interactions between CuO and ZrO_2, leading to improved dispersion of active sites and greater stability under reaction conditions [11, 12]. Furthermore, these NCPs are utilized in environmental applications such as the electrochemical reduction of CO_2 to ethylene, demonstrating high faradaic efficiency and current density, which are critical for sustainable energy solutions. The unique properties of CuO/ZrO_2 NCPs make them valuable in various fields, including energy storage, environmental remediation, and catalysts in chemical synthesis and industrial processes [12].

The literature indicates that mechanical alloying [1, 2], hydrothermal processes [13], sol-gel methods [14], and electrospinning [13, 15, 16] can be used to prepare metal-doped composites. After these production methods, powders are compacted and sintered. Sintering has been conducted in various ways over the last decade, including CS, microwave sintering [4], spark plasma sintering (SPS) [17], and FS [16]. Using these sintering techniques CuO/ZrO_2 NCPs can be used in various applications, including photocatalytic degradation, wear resistance, and improvement of electrical conductivity. Despite the use of other ceramic materials to enhance the properties of ZrO_2, research on integrating a very fine grain structure into CuO and exploring its physical, microstructural, and sintering techniques remains limited.
This study investigated the effect of CS and FS on the microstructures and densities of CuO/ZrO_2 NCPs produced by the hydrothermal method in a 1:1 weight ratio, providing insights for future research. CS of CuO/ZrO_2 NCPs requires several hours at 1200 to 1500°C to achieve full density [18]. However, FS offers a mechanism for achieving similar results at lower temperatures in shorter periods. Additionally, a comparison of FS and CS effects on CuO/ZrO_2 NC microstructures and density has not yet been reported. To the best of the authors' knowledge, this study is the first report to explore this comparison of the CuO/ZrO_2 NCPs densification.

2.2. Materials And Methods

2.1. Materials

Zirconium (IV) nitrate pentahydrate ($Zr(NO_3)_4.5H_2O$, China) and sodium oleate (NaOL, $CH_3(CH_2)_7CH$, China) were used for the production of ZrO_2 NPs. Urea ($Co(NH_2)_2$, Sigma Aldrich) and copper (II) nitrate hydrate ($Cu(NO_3)_2.2.5H_2O$, Sigma Aldrich) were purchased for the production of the CuO particles. Ammonia was purchased to adjust pH and used for synthesizing both particles. Distilled water was utilized for hydrothermal synthesis.

2.2. Synthesis of CuO/ZrO_2 NCPs

In the previous study, CuO/ZrO_2 NCPs were produced by hydrothermal synthesis [15]. Briefly, this synthesis has two steps and is schemed in Figure 1. First, in two separate beakers, $Zr(NO_3)_4.5H_2O$ (metal source) was dissolved in 30 ml and NaOL (surfactant) in 15 ml of water mixed in a 1/2 volume ratio for 10 minutes at room temperature. The solution pH was adjusted to 9.4 with NH_3, and the white precipitate became homogeneous. Then, in two separate beakers, 0.1 M $Cu(NO_3)_2.2.5H_2O$, and urea were dissolved in 50 ml of water and stirred for 15 minutes. After mixing solutions, the pH was adjusted to 9.4. The two solutions were stirred in a 1/1 volume ratio for 10 minutes. The final solution was transferred to the hydrothermal unit at room temperature and heated at 200 °C for 13 hours. In the second step of this process, after 13 hours at 200 °C, the autoclave was cooled down to room temperature. Black precipitation was washed with water, ethanol, and acetone and

heat-treated at 600 ºC for 3 hours. Additionally, each NP (ZrO_2 and CuO) solution can be prepared individually using the same procedure.

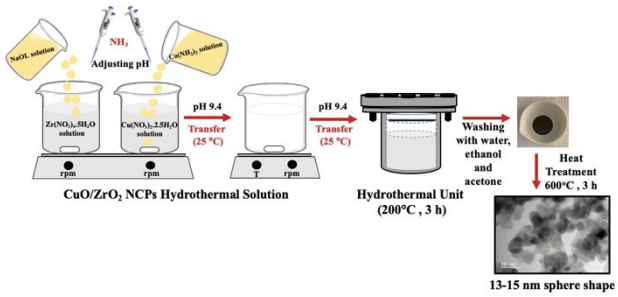

Figure 1. Scheme of the synthesis of the CuO/ZrO_2 NCPs

2.3. Preparation of the CuO/ZrO_2 NCPs pellets

The CuO/ZrO_2 NCPs were pressed using a uniaxial press (Hidroliksan, 2013) to make identical pellets under 50 bar pressure. The pellet-type stainless steel die has a 13 mm diameter and 2 mm thickness. These green-density pellet samples of the CuO/ZrO_2 NCPs were prepared and used in the CS and FS stages.

2.4. CS and FS methods

One of these samples was prepared for the CS. CS was performed for 1 hour in a furnace (Protherm, PLF 130/10) heated to 1250 °C with a heating rate of 3 °C /min.

A power source (Ametek, XG600-2.6) was used for the FS experiment to apply the DC electric field with the current control system. The maximum current was applied from the DC power source. The computer-aided system recorded the electric field and current flow (Fig. 2). The pellet was positioned in a parallel plate capacitor experimental setup, a sandwich form for FS. The FS setup details have been mentioned frequently in our previous studies [16, 19-21]. The pellet was placed, and the wires were attached to the power source. A quartz glass window settled on the front of the furnace to record the FS experiment.

The FS experiment furnace was programmed to increase the temperature to 800 °C with a heating rate of 15 °C /minute. When the flash started, the furnace temperature paused and was kept at that temperature. The graph was plotted using data obtained just before the flash started. (The data collected until the furnace temperature reached 673 °C were not included in the graph). The power supply (DC) generates an electric field of chosen voltages to trigger the flash of the CuO/ZrO_2 NCPs pellet. With the previous experience, the cut-off value was 50 mA/mm^2 to minimize joule heating and avoid thermal runaway. Thanks to the current draw by the pellet would lead to joule heating, the internal temperature of the pellet was increased over the furnace temperature. This study has determined the current cut-off and electric field values.

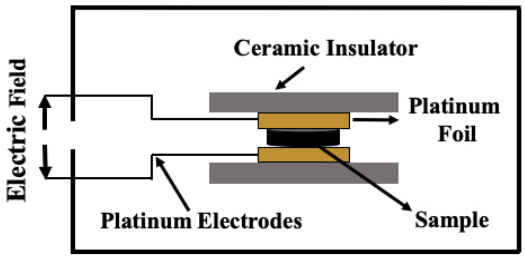

Figure 1. Parallel plate capacitor type of FS experiment setup [19]

2.5. Characterization

After the CS and FS experiments, the first phase structure was checked from the X-ray diffraction analysis (XRD, Europe 600 Benchtop XRD Instrument, Cu-Kα, λ=1.54 Å) in the range of 10-100° and the scanning speed was 2 °/min. Then, the morphology of the before-sintering (green) CuO/ZrO_2 NCP sample was examined by transmission electron microscopy (TEM, JEOL-JEM 2100). Using scanning electron microscopy (SEM, Zeiss LS- 10) equipped with an energy dispersive X-ray spectroscopy (EDX) analysis was conducted on a gold-coated cross-sectional area of the CuO/ZrO_2 NCPs pellet sample for the study of the after CS and FS experiment microstructures. After that, green, CS, and FS sample densities were measured using the Archimedes method.

3. Results and Discussion

The XRD pattern of the CuO/ZrO_2 NCPs after heat treatment at 600 °C is presented in Figure 3. It is proven that, after heat treatment, a mixture of CuO and ZrO_2 was achieved. The CuO and ZrO_2 phases remain unchanged. The previous

study showed that ZrO_2 peaks have broader intensity values than CuO peaks and ZrO_2 NPs are smaller than CuO particles [15].

The ZrO_2 and CuO-doped ZrO_2 NCPs crystallite sizes were determined to be 8.8 and 12.3 nm by the Debye-Scherrer formula, respectively.

$$D = (k\,\lambda)/\beta\cos\theta \quad (1)$$

In this equation, where D is the grain size, λ is the wavelength of X-ray diffraction (λ= 1.5404 Å), K= 0.9 which is the correction factor, β is FWHM of the most intense diffraction factor (calculated with Origin software), and θ is the Bragg angle.

The shape and size of the CuO/ZrO_2 NCPs were investigated by TEM (Fig. 4), which are illustrated to be spherical-shaped, with a particle size of between 13-15 nm. This production method produces smaller particles than other methods, such as mechanical alloying [5].

Fine particles are good for forming composites because they have suitable dislocation for movement barriers and can be uniformly dispersed at inter-particle boundaries [22]. Similarly, spherical-shaped ceramic particles resulted in better bonding than irregular ones for Cu/ZrO_2 composites [13, 14].

The high-resolution transmission electron microscopy (HR-TEM) inset in Fig. 4 reveals that a spherical shape and 14.6 nm maximum particle size were produced with this NCP procedure. Furthermore, the inset of Fig. 4 exhibits that the interplanar spaces are uniform and 1.3 Å.

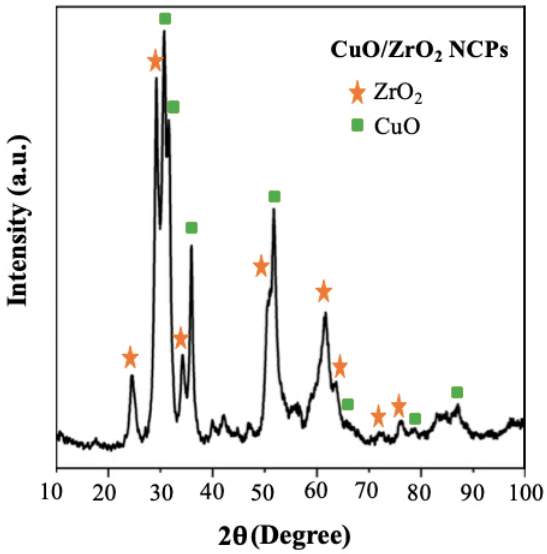

Figure 3. XRD pattern of the as-synthesis of the CuO/ZrO_2 NCPs

The 100 V/cm electric fields were applied to the CuO/ZrO_2 NCPs pellet in a parallel plate capacitor geometry. The current was kept constant at 50 mA/mm^2 to be sure the current density was not exceeded. The sample was heated to 800 °C with a 15 °C /min heating rate. The current-voltage data was recorded as a function of time.

The electric field-assisted system is described in three stages. Stage I is incubation, Stage II is the transition stage, and Stage III is the steady state. Stage I shows no current draws until flash starts and Stage II shows the current's cut-off value. At Stage III, the current control of the power supply is maintained (Fig. 5).

CuO/ZrO_2 NCP pellet under the 100 V/cm applied field showed no current draw until the furnace reached 670 °C (Stage I). At the end of Stage I, the sample showed insulator behavior (between 25 °C and 670 °C). The current leakage was detected as 1.6 mA/mm^2 during this stage. When the furnace reached 673 °C, the current had a maximum point of 50 mA/mm^2, and the electric field decreased to 40 V/cm. As the flash began 673 °C, the furnace temperature was paused and maintained at a constant level. This allowed for the measurement of the sample temperature during the flash process. In the graph part of the incubation stage was shown and finished in less than 28 seconds.

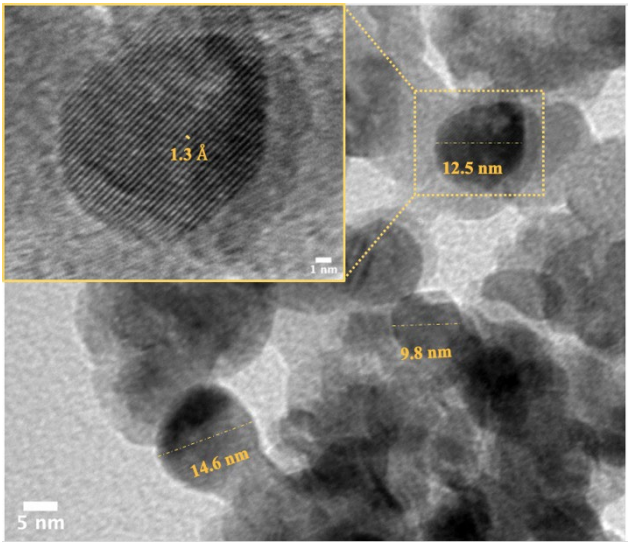

Figure 4. TEM images of the CuO/ZrO_2 NCPs (the inset on the left side of the figure presents the magnification of the circled area)

At Stage II, the sample conductivity started to increase. Furthermore, the transition stage showed a rapid increase in the current draw at 673 °C. The DC power source was changed from voltage control to a current control system to avoid excessive Joule heating. At that time, the sample had a maximum power absorption at this stage of the FS. After the flash, the sample temperature reached at 773 °C in 15 seconds. Overpower absorption could lead to high Joule heating, causing abnormal grain growth, which is not recommended. The Stage III of this experiment is to retain the current control of the power supply. The power source shut down within 30 seconds when the current density was stabilized. FS (Stage II), spanning 15-20 seconds during Stage III, is believed to be part of the FS process.

The FS experiment was completed in 60 seconds with three stages. In the literature, at least 1 hour of production time at 1250 °C is required for the CS process in CuO/ZrO_2 NCPs [23]. The method used in this study reduced the sintering temperature by 577 °C and the sintering time to 60 seconds with electric field assisted/FS.

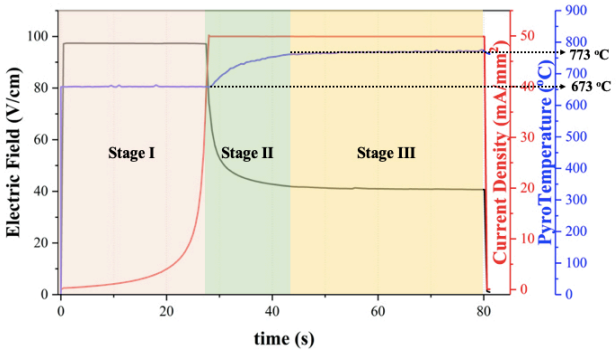

Figure 5. FS experiment of CuO/ZrO_2 NCPs under 100 V/cm electric field at 673 °C furnace temperature

The FS energy consumption of the CuO/ZrO_2 NCPs is approximately 2.2 kJ, corresponding to an energy density consumption of 0.227 kJ/cm³. In contrast, CS samples in the same furnace consume around 13 kJ per unit, which corresponds to an energy density consumption of 54 kJ/cm³. Thus, the energy consumption of the flash-sintered sample was approximately six times lower than that of the sample sintered using the conventional method. The FS method shows promise for producing CuO/ZrO_2 NCPs in future applications, particularly concerning carbon emission reduction and energy saving.

Figure 6 represents the microstructure morphology of the conventional and flash-sintered samples taken from the cross-sectional area. SEM micrographs taken from the cross-sectional area of the CuO/ZrO_2 NCPs material for CS are shown in Figure 6a.

The orange dashed area inset of Fig. 6a was given as the magnified area of the selected. Besides, Figs. 6c and 6d show the elemental mapping of the orange dashed line area in Figs. 6a and 6b, respectively. Furthermore, the EDX spectrum in Figs. 6c and 6d reveal that the sample comprises Cu, Zr, and O elements. Fig. 6a observes that the intergranular boundaries do not disappear with CS, and the sintering process does not take place sufficiently. The microstructure shows the formation of a less porous, high-density structure, confirming the density measurement with the FS pellet (Fig. 6b). After the sample was brought to room temperature, the density was measured according to Archimedes' principle.
The density for the green, conventional, and flash-sintered samples was measured as 2.92, 3.72, and 4.38 g/cm^3, respectively. FS has been

demonstrated to decrease grain size, resulting in a higher density compared to samples sintered using conventional methods. Moreover, with this value, it was proven that the sintering process obtained from the SEM micrograph was successful and convenient. These values were very reasonable compared to the literature [1-3, 22].

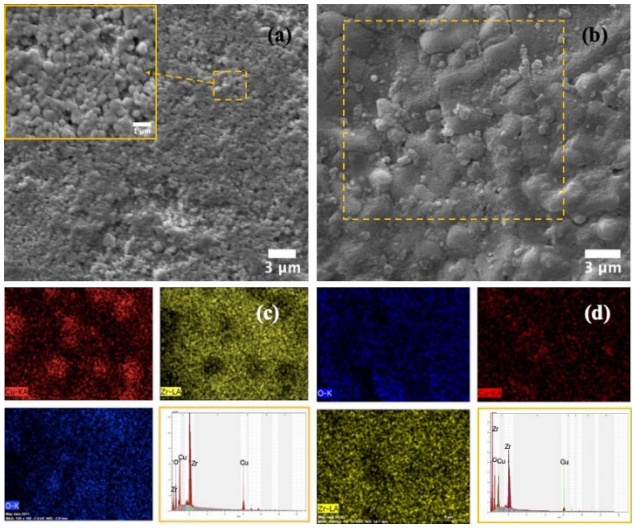

Figure 6. SEM micrograph of a) conventional, b) flash-sintered CuO/ZrO_2 NCPs and EDS and EDX analysis of c) CS and d) FS sample selected areas

4. Conclusion

This study was compared with an applied electric field-assisted/FS and CS technique to obtain highly dense CuO/ZrO_2 NCPs. The best authors' knowledge from the literature, FS of CuO/ZrO_2 NCP material has yet to be studied. Thus, this study is *the first report* on this material using the FS method.

The CuO/ZrO_2 NCP pellet sample was exposed to an electric field of 100 V/cm with a current density of 50 mA/mm^2, and no current draw was recorded in the experimental system. The maximum current density was achieved at 673 °C, and the power supply was self-regulated by the electric field-current relationship. Furthermore, in the flash experiment, the system measured the sample temperature of ~737 °C.

The CS of the CuO/ZrO_2 NCPs pellet was sintered at 1250 °C for 1 hour. The density of the green, CS, and FS of the CuO/ZrO_2 NCPs samples was measured by the Archimedes method as 2.92, 3.72, and 4.38 g/cm^3, respectively. In light of the SEM micrographs, the grain boundaries cannot disappear with CS. However, the FS experiments allow for obtaining denser microstructures than those obtained with CS. The density results of the CS and FS pellets confirmed the SEM micrograph images. This experimental procedure reduced the sintering temperature by 577 °C and the processing time from 1 hour to 60 seconds for producing products with CuO/ZrO_2 NCPs at lower temperatures and resulted in a denser structure. The FS process significantly reduces energy consumption, requiring about six times less energy than the CS method. This makes FS a promising technique for producing CuO/ZrO_2 NCPs, especially in applications where reducing carbon emissions and energy saving are the priorities.

Article Information Form

Acknowledgments
The author would like to thank TUBITAK 2219-International Postdoctoral Research Fellowship Program for supporting her research at the University of Colorado at Boulder.

Funding
The author gratefully acknowledges the financial support provided by the Scientific Research Projects Coordination Unit of Konya Technical University (Contract # BAP- 211019030) for the examining the samples.

The Declaration of Conflict of Interest/ Common Interest
No conflict of interest or common interest has been declared by the author.

The Declaration of Ethics Committee Approval
This study does not require ethics committee permission or any special permission.

The Declaration of Research and Publication Ethics
The author of the paper declare that they comply with the scientific, ethical and quotation rules of SAUJS in all processes of the paper and that they do not make any falsification on the data collected. In addition, they declare that Sakarya University Journal of Science and its editorial board have no responsibility for any ethical violations that may be encountered, and that this study has not been evaluated in any academic

publication environment other than Sakarya University Journal of Science.

References

[1] A. Fathy, O. Elkady, A. Abu-Oqail, "Production and properties of Cu-ZrO_2 nanocomposites," Journal of Composite Materials, vol. 52, no. 11, pp. 1519–1529, 2018.

[2] Y. Sakka, T. S. Suzuki, K. Ozawa, T. Uchikoshi, K. Hiraga, "Sintering and ionic conductivity of CuO-doped tetragonal ZrO_2 prepared by novel colloidal processing," Journal of the Ceramic Society of Japan, vol. 109, no. 1276, pp. 1004–1009, 2001.

[3] A. Fathy, A. Wagih, A. Abu-Oqail, "Effect of ZrO_2 content on properties of Cu-ZrO_2 nanocomposites synthesized by optimized high energy ball milling," Ceramics International, vol. 45, no. 2, pp. 2319–2329, 2019.

[4] P. S. Selvamani, J. Judith Vijaya, L. John Kennedy, A. Mustafa, M. Bououdina, P. Joice Sophia, R. Jothi Ramalingam, "Synergic effect of Cu_2O/MoS_2/rGO for the sonophotocatalytic degradation of tetracycline and ciprofloxacin antibiotics," Ceramics International, vol. 47, no. 3, pp. 4226–4237, 2021.

[5] Y. A. Sorkhe, H. Aghajani, A. Taghizadeh Tabrizi, "Mechanical alloying and sintering of nanostructured TiO_2 reinforced copper composite and its characterization," Materials & Design, vol. 58, pp. 168–174, 2014.

[6] M. K. G. Abbas, S. Ramesh, K. Y. Sara Lee, Y. H. Wong, C. Y. Tan, U. Johnson Alengaram, P. Ganesan, F. Musharavati, and E. Zalnezhad "Densification of copper oxide doped alumina toughened zirconia by conventional sintering," Ceramics International, vol. 48, no. 5, pp. 6287–6293, 2022.

[7] S. Azhar, K. S. Ahmad, I. Abrahams, W. Lin, R. K. Gupta, A. El-marghany, "Synthesis of phyto-mediated CuO–ZrO_2 nanocomposite and investigation of their role as electrode material for supercapacitor and water splitting studies," Journal of Materials Research, vol. 22, pp. 4937–4950, 2023.

[8] M. Shojaei, A. Hasani, Z. Amiri, G. R. Khayati, "Using the group method for the synthesis of copper/ZrO_2 nanocomposites to achieve high wear resistance by ball milling and spark plasma sintering," Ceramics International, vol. 48, no. 12, pp. 17576–17588, 2022.

[9] S. G. Giniyatova, N. A. Sailaukhanov, E. Nesterov, M. V. Zdorovets, A. L. Kozlovskiy, D. I. Shlimas, "Research of Structural, Strength and Thermal Properties of ZrO_2-CeO_2 Ceramics Doped with Yttrium," Crystals, vol. 12, no. 2, p. 242, 2022.

[10] A. H. Shukor, H. A. Alhattab, I. Takano, "Electrical and optical properties of copper oxide thin films prepared by DC magnetron sputtering," Journal of Vacuum Science & Technology B, vol. 38, no. 1, p. 012803, 2019.

[11] S. N. Basahel, M. Mokhtar, E. H. Alsharaeh, T. T. Ali, H. A. Mahmoud, K. Narasimharao, "Physico-Chemical and Catalytic Properties of Mesoporous CuO-ZrO_2 Catalysts," Catalysts, vol. 6, no. 4, 2016.

[12] P.-P. Guo, Z.-H. He, S.-Y. Yang, W. Wang, K. Wang, C.-C. Li, Y.-*Y.* Wei, Z.-T. Liu, B. Han, "Electrocatalytic CO_2 reduction to ethylene over ZrO_2/Cu-Cu_2O catalysts in aqueous electrolytes," Green Chemistry, vol. 24, no. 4, pp. 1527–1533, 2022.

[13] İ. C. Kaya, Ç. Çetin, H. S. Aydın, M. S. Yavuz, B. Z. Büyükbekar, M. Uyaner, V.

Kalem, H. Akyıldız, "Production of $CuAlO_2$ in powder, bulk and nanofiber forms," Journal of Ceramic Processing Research, vol. 16, no. 5, pp. 648–655, 2015.

[14] J. Liu, J. Shi, D. He, Q. Zhang, X. Wu, Y. Liang, Q. Zhu "Surface active structure of ultra-fine Cu/ZrO_2 catalysts used for the CO_2+ H_2 to methanol reaction," Applied Catalysis A: General, vol. 218, no. 1–2, pp. 113–119, 2001.

[15] Z. Çetinkaya, "Production of CuO/ZrO_2 Nanocomposites in Powder and Fiber Forms," *KONJES*, vol. 12, no. 1, pp. 221–230, 2024.

[16] Z. Çetinkaya, E. Güneş, İ. Şavkliyildiz, "Investigation of biochemical properties of flash sintered ZrO_2–SnO_2 nanofibers," Materials Chemistry and Physics, vol. 293, p. 126900, 2023.

[17] J. Baneshi, M. Haghighi, N. Jodeiri, M. Abdollahifar, H. Ajamein, "Homogeneous precipitation synthesis of CuO–ZrO_2–CeO_2–Al_2O_3 nanocatalyst used in hydrogen production via methanol steam reforming for fuel cell applications," Energy Conversion and Management, vol. 87, pp. 928–937, 2014.

[18] Z. A. Hamid, "Composite and nanocomposite coatings," Journal of Metallurgical Engineering, vol. 3, no. 1, pp. 29–42, 2014.

[19] Z. Çetinkaya, "Flaş sinterleme yönteminin uçucu kül mikroyapısına etkisi," Journal of The Faculty of Engineering and Architechure of Gazi University, vol. 37, no. 1, pp. 137–144, 2021.

[20] Z. Çetinkaya, A. Gökhan, S. Dursun, İ. Şavkliyildiz, "Reusing blended leach residue by flash sintering method," International Journal of Applied Ceramic Technology, vol. 21, pp. 1567-1573, 2024.

[21] Z. Çetinkaya, "Investigation of Reusing Copper Converter Slag Residue with the Flash Sintering Method," JOM, vol. 75, no. 12, pp. 5361–5371, 2023.

[22] W. Li, H. Assadi, F. Gaertner, S. Yin, "A Review of Advanced Composite and Nanostructured Coatings by Solid-State Cold Spraying Process," Critical Reviews in Solid State and Materials Sciences, vol. 44, no. 2, pp. 109–156, 2019.

[23] M. Khaloobagheri, B. Janipour, N. Askari, E. Shafiee Kamal Abad, "Characterisation of powder metallurgy Cu-ZrO_2 composites," Advances in Production Engineering And Management, pp. 242–248, 2013.